Activation of a bacterial flow sensor by hypochlorous acid from stimulated neutrophils

Ilona P. Foik[1,†], Lauren A. Urban[2-4,†], Andy P. Huang[5], Timothy L. Downing[2-4,6,*], Albert Siryaporn[1,5,*]

[1]Department of Physics & Astronomy, University of California Irvine; Irvine, California, USA.

[2]Department of Microbiology & Molecular Genetics, University of California Irvine; Irvine, California, USA.

[3]NSF-Simons Center for Multiscale Cell Fate, University of California Irvine; Irvine, CA, USA.

[4]UCI Edwards Lifesciences Foundation Cardiovascular Innovation and Research Center (CIRC), University of California Irvine; Irvine, CA, USA.

[5]Department of Molecular Biology & Biochemistry, University of California Irvine; Irvine, California, USA.

[6]Department of Biomedical Engineering, University of California Irvine, Irvine; California, USA.

[†]These authors contributed equally.

[*]To which correspondence should be sent:
T. Downing: tim.downing@uci.edu
A. Siryaporn: asirya@uci.edu

ABSTRACT

Bacteria sense environmental stressors and activate responses to improve their survival in harsh growth conditions. Neutrophils respond to the presence of bacteria by producing oxidative antibacterial species including hypochlorous acid (HOCl). However, the extent that bacteria detect activated neutrophils or HOCl has not been known. Here, we report that the opportunistic bacterial pathogen *Pseudomonas aeruginosa* responds to activated neutrophils by activating the *fro* system, which regulates the expression of antioxidative factors. We show that this response is specific to HOCl and that other oxidative factors including H_2O_2, do not trigger a *fro* response. The *fro* system has been previously shown to detect flow that is present in host vasculature, such as in animal circulatory systems. Our data thus suggest a model in which *fro* serves as an early host detection system in *P. aeruginosa* that improves its survival against neutrophil-mediated defenses, which could promote colonization in human tissue and increase pathogenicity.

One Sentence Summary: *P. aeruginosa* primes its defenses against neutrophils by sensing flow and hypochlorous acid via the *fro* system.

21 **INTRODUCTION**

22 *P. aeruginosa* is a Gram-negative bacterium that is a major cause of acute hospital-
23 acquired infections and a significant threat for antibiotic-resistant infections *(1)*. To survive in a
24 broad range of conditions, this bacterium has evolved signaling pathways that relay information
25 about changes in nutrients, chemical gradients, and mechanical forces such as those generated by
26 flow, and stimulates responses that promote survival *(2, 3)*. Many of these signaling pathways
27 improve the bacterium's survival in hosts in particular. Understanding how such environmental-
28 sensing pathways detect and respond to host cues is critical for improving treatments of bacterial
29 infections.

30 Mammalian host immune systems respond to the presence of bacterial pathogens by
31 recruiting immune cells to sites of infection. Neutrophils are among the first and most abundant
32 immune cells recruited to inflamed or damaged tissues *(4)*. Neutrophils are stimulated into an
33 activated state by the presence of the bacterial components, including the membrane constituent
34 lipopolysaccharide. Activated neutrophils kill bacteria through a number of mechanisms,
35 including producing respiratory burst products such as reactive oxygen species (ROS) and
36 reactive chlorine species (RCS) *(5, 6)*. While the toxic effects of ROS on bacteria are understood,
37 far less is known about how bacteria are affected by RCS *(7, 8)*. Hypochlorous acid (HOCl) is a
38 major neutrophil RCS that has strong bactericidal activity towards bacteria *(9, 10)*. HOCl is
39 formed through the activity of myeloperoxidase with H_2O_2 and chlorine ions *(5, 6, 11)*. *P.*
40 *aeruginosa* is a potent activator of neutrophil respiratory bursts *(12)*. However, whether and how
41 *P. aeruginosa* detects and responds to neutrophil respiratory bursts is not understood.

42 Recently, it was reported that *P. aeruginosa* detects the flow of fluids via the flow-
43 regulated operon *fro (3)*. Flow is ubiquitous in the lung and in the circulatory system, which

44 neutrophils and other immune cells must travel through to reach infected sites. The *fro* system
45 could thus enable *P. aeruginosa* to detect the presence of flow-associated host environments and
46 immune system components. *P. aeruginosa* induces *fro* operon expression during infections in
47 humans *(3, 14)* (Fig. 1A).The operon consists of the genes *froABCD* (*PA14_21570*,
48 *PA14_21580, PA14_21590, PA14_21600*). FroB is predicted to localize in cytoplasm while FroC
49 and FroD are predicted to localize to the inner membrane *(15)*. The *fro* operon is regulated by
50 two upstream genes, *froR* (*PA14_21550)* and *froI* (*PA14_21560*), which are sigma and anti-
51 sigma factors, respectively *(16)*. Overexpression of *froR* increases *fro* expression whereas
52 overexpression of *froI* eliminates *fro* induction *(3)*. Flow activates FroR-dependent transcription
53 of *froABCD* through an unknown mechanism.
54 We investigated whether the *fro* system directly responds to components of the
55 circulatory system. Here, we show that the expression of the *fro* system is upregulated by
56 activated neutrophils. We determine that HOCl is a critical component of the neutrophil
57 activation that is responsible for the *fro* upregulation and that its upregulation reduces the
58 bactericidal effects of HOCl. These data suggest a novel mechanism by which a bacterial defense
59 system is primed to detect host immune system activity through both flow and the presence of
60 the immune cell effector HOCl, and responds by producing protective antioxidant proteins.

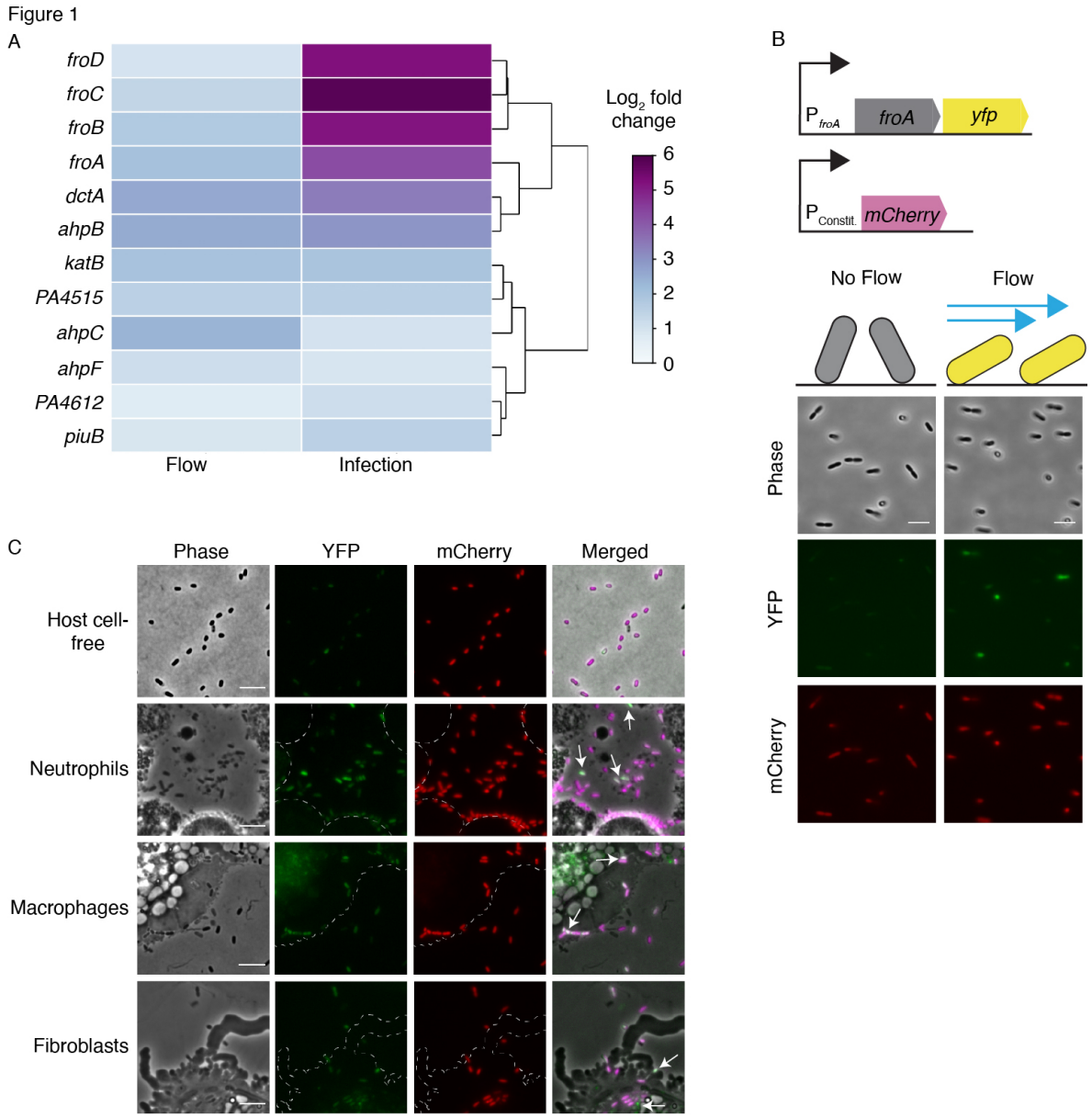

Fig. 1 Activation of *fro* transcription by flow and during infection of human tissue. (A) RNA-seq heatmap of *P. aeruginosa* genes that are significantly upregulated at least 3-fold both by flow and during infections in human wounds. RNA-seq datasets are from *(3, 14)*. **(B)** Top: schematic of a *P. aeruginosa* fluorescent reporter strain that contains a transcriptional fusion of *yfp* to *fro* and constitutively expresses *mCherry*. Representative phase contrast, YFP, and mCherry images the reporter under flow (right) or non-flow (left) conditions for 30 minutes. **(C)** Representative phase contrast, YFP, mCherry, and merged images of the *P. aeruginosa* reporter strain co-incubated with neutrophils, macrophages, fibroblasts, or host cell-free media for 30 minutes. Dotted lines outline the boundaries of the host cells. White arrows in merged images indicate *P. aeruginosa* with the high ratios of YFP/mCherry intensities. Images are representative of three independent repetitions. Scale bars represent 5 µm.

74 **RESULTS**

75 **Host cells stimulate *fro* expression in *P. aeruginosa* under non-flow conditions**

76 We investigated if the *fro* operon is activated directly by immune cells. To quantify *fro*
77 expression, we used a *P. aeruginosa* strain that co-expresses the yellow fluorescent protein
78 (YFP) under the transcriptional control of the *fro* promoter and mCherry under the control of a
79 constitutive promoter (Fig. 1B). Neutrophils and macrophages are among the first immune cells
80 that are recruited to sites of infection. We co-incubated *P. aeruginosa* with these cells for 30
81 minutes to determine whether they would elicit a response in the *fro* operon. Experiments were
82 performed in the absence of flow in order to deconvolve the effects of flow from potential
83 activation of *fro* by host cells. Relative to *P. aeruginosa* that were incubated in host cell-free
84 media, *P. aeruginosa* in close proximity to neutrophils or that were engulfed in macrophages had
85 higher levels of *fro* expression (Fig. 1C). Furthermore, increases in *fro* expression were observed
86 in some *P. aeruginosa* that were internalized in fibroblasts (Fig. 1C). These data suggest direct
87 interaction or close proximity with host hosts stimulates *fro* expression in *P. aeruginosa*.

88

89 ***fro* expression is induced by activated neutrophils**

90

91 We focused our efforts on understanding how neutrophils activate *fro* expression, as
92 neutrophils are one of the first immune cells that are recruited to bacterial infection sites.
93 *P. aeruginosa* triggers respiratory bursts in neutrophils *(12)*, which generates ROS and RCS. We
94 hypothesized that the observed *fro* activation could be a response to respiratory burst products.
95 To test this, we determined whether molecules released by activated neutrophils could induce *fro*
96 expression. We isolated cell-free conditioned medium from neutrophils that were stimulated to
97 induce respiratory bursts using 100 ng/mL phorbol myristate acetate (PMA) in neutrophil

isolation medium (PBGT) *(17)*. *P. aeruginosa* were cultured for 3 hours in the conditioned medium (Fig. 2A). The expression of *fro* was quantified by computing the ratio of YFP to mCherry fluorescence in individual *P. aeruginosa* and averaging over at least one hundred *P. aeruginosa.* Conditioned medium from PMA-stimulated neutrophils increased the expression of *fro* by 30-fold compared to medium from unstimulated neutrophils (Fig. 2B). The upregulation in *fro* was not due to PMA, as the addition of PMA without neutrophils had no effect on *fro* expression (Fig. 2B). The conditioned media from unstimulated neutrophils had no significant effect on *fro* expression compared to PBGT medium alone (Fig. 2B).

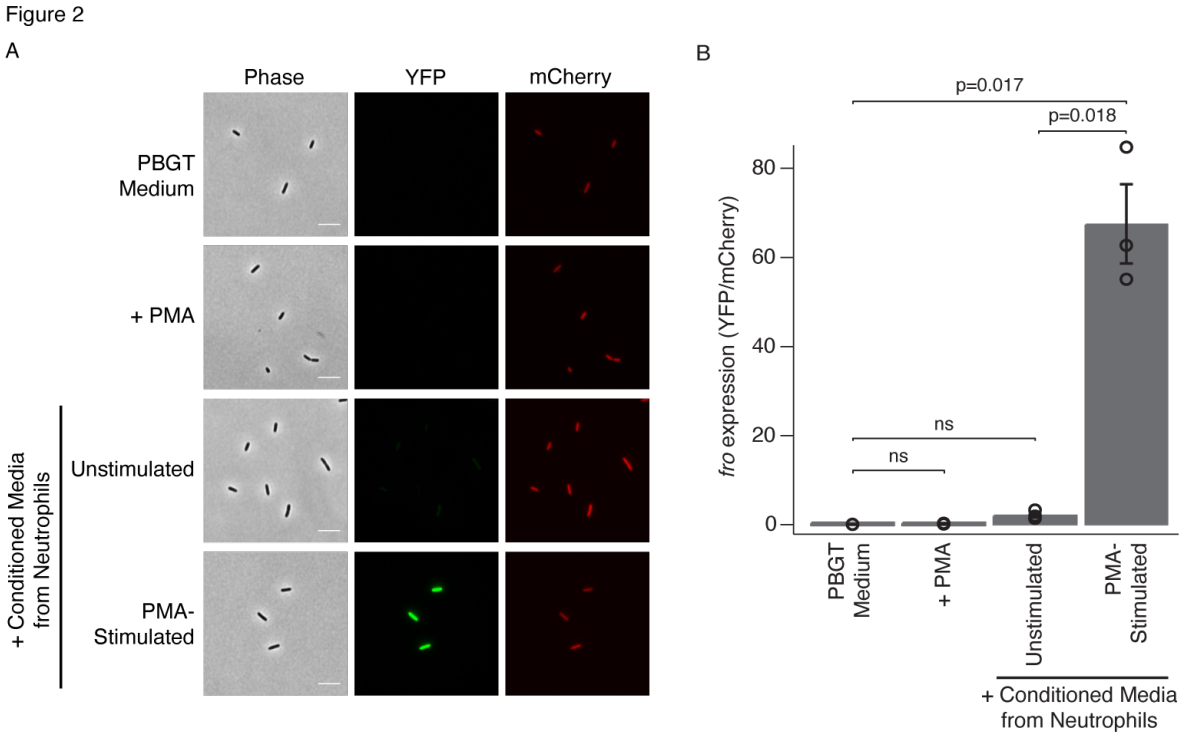

Fig. 2 Conditioned medium from stimulated neutrophils induces *fro* expression. (A) Representative phase-contrast and fluorescence images and **(B)** quantification of *fro* expression levels of *P. aeruginosa* that were cultured for 3 hours in PGBT medium with or without 100 ng/mL of PMA, conditioned medium from unstimulated neutrophils, or conditioned medium from neutrophils that were stimulated with 100 ng/mL of PMA. Bars indicate the mean and error bars represent the standard error of the mean (SEM) of three independent experiments. P-values were calculated using a two-tailed, unequal variance t-test. ns indicates $p > 0.05$. Scale bars represent 5 μm.

116 ***fro* expression is induced by HOCl but not by H_2O_2 or HNO_3**

117 We assessed the ability of specific respiratory burst products to drive *fro* activation.
118 Activated neutrophils generate multiple ROS and RCS oxidants, which have an inhibitory effect
119 on bacterial growth *(5–7, 9, 10)*. We hypothesized that these oxidants induce *fro* expression and
120 tested the impact of these species on *fro* expression at near-inhibitory concentrations (Fig. 3A).
121 We established that 1 μM of NaOCl or 8 μM of H_2O_2 were at the threshold of growth inhibition
122 for *P. aeruginosa* (Fig. 3B), and subsequently measured *fro* expression in cultures up to these
123 concentration thresholds. H_2O_2 in a range of concentrations below, at, or above 8 μM had no
124 significant impact on *fro* expression (Fig. 3C-D). In contrast, 1 μM NaOCl increased *fro*
125 expression by up 78-fold compared to untreated cultures. This activation is not due to sodium or
126 chloride ions alone, as neither NaCl at the same concentration or HCl up to the highest
127 concentration without changing pH of the minimal medium did not induce *fro* expression (Fig.
128 3D). In addition, the *fro* response to NaOCl is not due to basic pH alone, as treatment with 6 mM
129 NaOH, which adjusted the medium to the same pH as 1 uM NaOCl (pH 7.1), had no significant
130 impact on *fro* activation (Fig. 3D). NaOCl-induced *fro* expression occurred at concentrations
131 below those associated with growth inhibition (Fig. 3B-D). The activation of *fro* by NaOCl is
132 consistent with a recent transcriptional study that identified *fro* as a gene that is upregulated by
133 HOCl *(18)*. We note that a higher concentration of 2 μM NaOCl did not increase *fro* expression.
134 However, this concentration caused a significant decrease in cell size (Fig. S1 in Supplementary
135 Materials), indicative of cell stress that may have interfered with transcription.

Figure 3

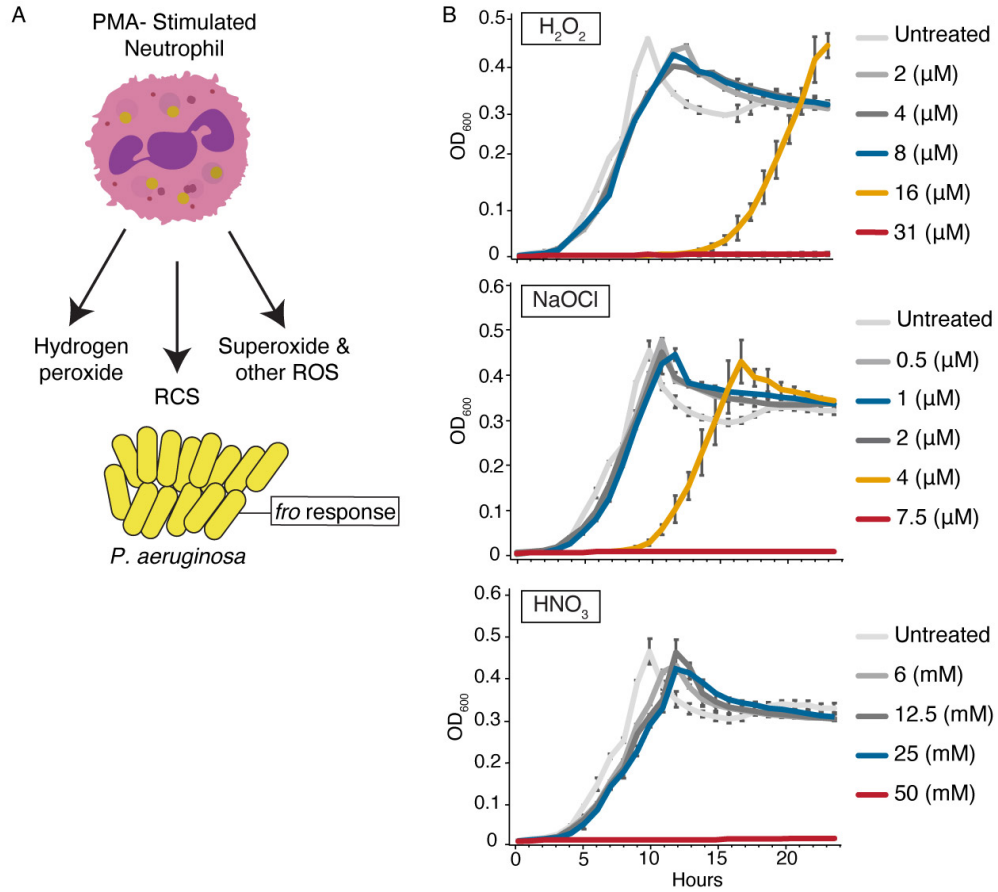
A
PMA- Stimulated Neutrophil
Hydrogen peroxide
RCS
Superoxide & other ROS
fro response
P. aeruginosa
B
H2O2
Untreated
2 (μM)
4 (μM)
8 (μM)
16 (μM)
31 (μM)
NaOCl
Untreated
0.5 (μM)
1 (μM)
2 (μM)
4 (μM)
7.5 (μM)
HNO3
Untreated
6 (mM)
12.5 (mM)
25 (mM)
50 (mM)
OD600
Hours

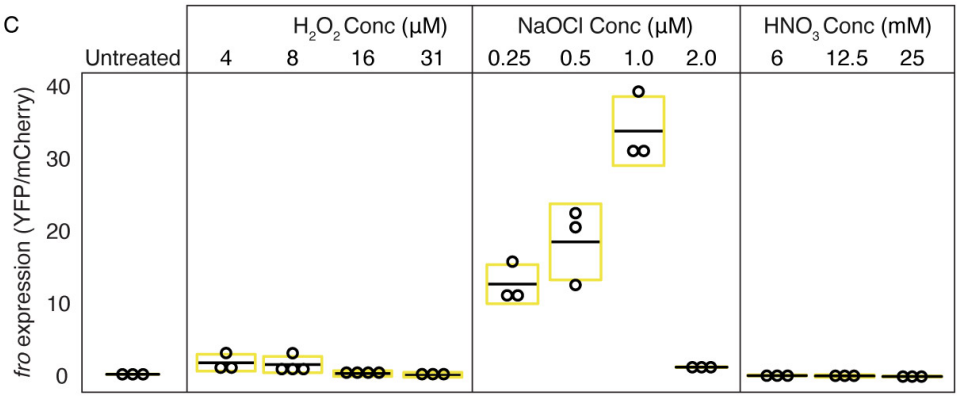
C
Untreated
H2O2 Conc (μM)
4
8
16
31
NaOCl Conc (μM)
0.25
0.5
1.0
2.0
HNO3 Conc (mM)
6
12.5
25
fro expression (YFP/mCherry)

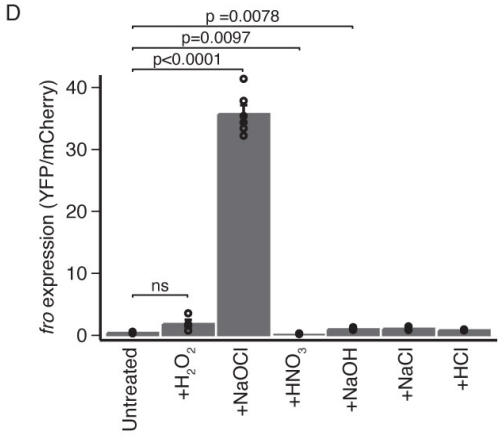
D
p =0.0078
p=0.0097
p<0.0001
ns
fro expression (YFP/mCherry)
Untreated
+H2O2
+NaOCl
+HNO3
+NaOH
+NaCl
+HCl

137 **Fig. 3 The expression of *fro* is induced by HOCl but not by H_2O_2 or HNO_3. (A)** Schematic of
138 model indicating that PMA-stimulated neutrophils produce respiratory burst products that could
139 induce *fro* expression. **(B)** Growth profiles, measured by optical density (OD_{600}), of
140 *P. aeruginosa* that were treated with sublethal and lethal concentrations of H_2O_2, NaOCl, HNO_3,
141 or untreated. Data points represent the mean and error bars indicate the SEM of at least two
142 independent experiments. **(C)** The expression of *fro* in *P. aeruginosa* that were treated for 3
143 hours with sublethal concentrations of H_2O_2, NaOCl, HNO_3, or were untreated. **(D)** The
144 expression of *fro* in *P. aeruginosa* that were treated for 3 hours with 8 μM H_2O_2, 1 μM NaOCl,
145 25 mM HNO_3, 6 mM NaOH, 1 μM NaCl, 200 μM HCl, or untreated. Bars represent the mean
146 and error bars indicate the SEM of at least two independent experiments. Boxplots indicate the
147 mean (black line) and interquartile range (yellow) of three independent experiments. P-values
148 were calculated using a two-tailed, unequal variance t-test. ns indicates $p > 0.05$.
149

150 We further assessed whether *fro* expression could be activated by the strong oxidant
151 HNO_3. The effects of this oxidizer were measured up to inhibitory concentrations (Fig. 3B-D).
152 However, no impact on *fro* expression was detected. These results suggest that *fro* responds
153 specifically to RCS stress from HOCl and supports the hypothesis that HOCl produced by
154 stimulated neutrophils activates *fro* expression.
155

156 **Antioxidant supplements inhibit *fro* activation**

157 HOCl oxidizes amine and sulfur groups within amino acids *(19, 22)*. We posited that
158 blocking the oxidative activity of HOCl could inhibit *fro* activation. Sulfur-containing amino
159 acids (e.g., methionine and cysteine) and beta-mercaptoethanol (βME) are antioxidants and
160 major targets for HOCl-mediated oxidation *(21, 23)*. We hypothesized that supplementing 1 μM
161 NaOCl treatments with methionine, cysteine, or βME reduces *fro* expression. Indeed, we
162 observed that supplementing these antioxidants at equal or lower concentrations as NaOCl (1 μM
163 methionine, 0.1 μM cysteine, or 1 μM βME) significantly reduced the NaOCl-induced *fro*
164 expression (Fig. 4A, Fig. S2 in Supplementary Materials) indicating that the oxidative activity of
165 NaOCl activates *fro*. Concentrations of antioxidants that were higher than 1 μM also inhibited

166 *fro* expression (Fig. S2 in Supplementary Materials). Treatments of cysteine, methionine, and
167 βME alone had no significant impact on *fro* expression (Fig. S3 in Supplementary Materials).
168 Based on these data, we hypothesized that the activation of *fro* expression by PMA-
169 stimulated neutrophils is suppressed by antioxidants. Indeed, we found that supplementing
170 conditioned media from PMA-stimulated neutrophils with 100 μM of methionine inhibited *fro*
171 activation (Fig. 4B) comparable to that observed in PBGT media alone and in unstimulated
172 neutrophils (Figs. 2B and 4B). Together, these results suggest that stimulated neutrophils activate
173 *fro* expression through the oxidative activity of HOCl.
174

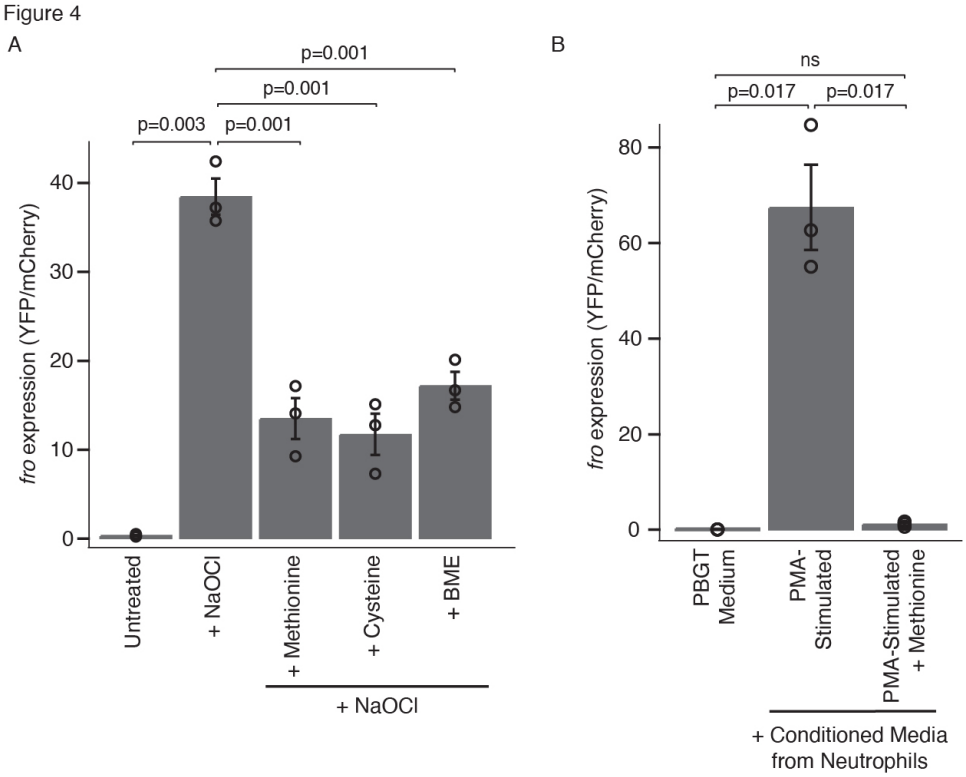

175

176 **Fig. 4 Antioxidants inhibit *fro* activation that is induced by HOCl and conditioned media**
177 **from PMA-stimulated neutrophils. (A)** The expression of *fro* in *P. aeruginosa* that are untreated,
178 treated with 1 μM NaOCl, or treated with 1 μM NaOCl and supplemented with 1 μM methionine,
179 0.1 μM cysteine, or 1 μM beta-mercaptoethanol (BME), for 3 hours. **(B)** Quantification of *fro*
180 expression levels in *P. aeruginosa* that were cultured in PBGT medium or in PBGT medium from
181 PMA-stimulated neutrophils (replotted from Fig. 2B) that was untreated or supplemented with

182 100 μM methionine. Bars represent the mean and error bars indicate the SEM of three independent
183 experiments. P-values were calculated using a two-tailed, unequal variance t-test. ns indicates
184 $p > 0.05$.
185

186 ***fro* enhances *P. aeruginosa* survival against HOCl**

187 We investigated whether *fro* activation has a beneficial impact on *P. aeruginosa* survival
188 in response to HOCl-induced stress. We measured the growth of wild-type *P. aeruginosa* and the
189 mutant strain Δ*froR*, which lacks the sigma factor that is required for *fro* activation. In the
190 absence of NaOCl, both strains grew comparably. Treatment with 16 μM NaOCl significantly
191 inhibited the growth of the wild-type strain (Fig. 5A). This treatment resulted in even greater
192 growth inhibition in the Δ*froR* strain. This result suggests that activation of the *fro* operon
193 increases *P. aeruginosa* survival against oxidative stress induced by HOCl.

194 We assessed the transcriptional pathways induced by *fro* activation to understand how *fro*
195 activation promotes the survival of *P. aeruginosa* during oxidative stress. We performed a Gene
196 Ontology (GO) analysis of RNA-seq data from the wild-type strain and Δ*froR* mutant *(3)*. This
197 analysis revealed that 128 genes with oxidoreductase activity were upregulated by at least 2-fold
198 in the wild-type strain compared to the Δ*froR* mutant (Supplemental Spreadsheet 1 in
199 Supplementary Materials). The most upregulated genes included *ahpC*, *ahpF*, and *katB*, which
200 encode proteins with oxidoreductase or antioxidant activity (Fig. 5B and Supplemental
201 Spreadsheet 2 in Supplementary Materials). These results suggest that *fro* activation promotes *P.*
202 *aeruginosa* survival against HOCl stress by activating transcriptional responses that mitigate
203 oxidative damage.
204

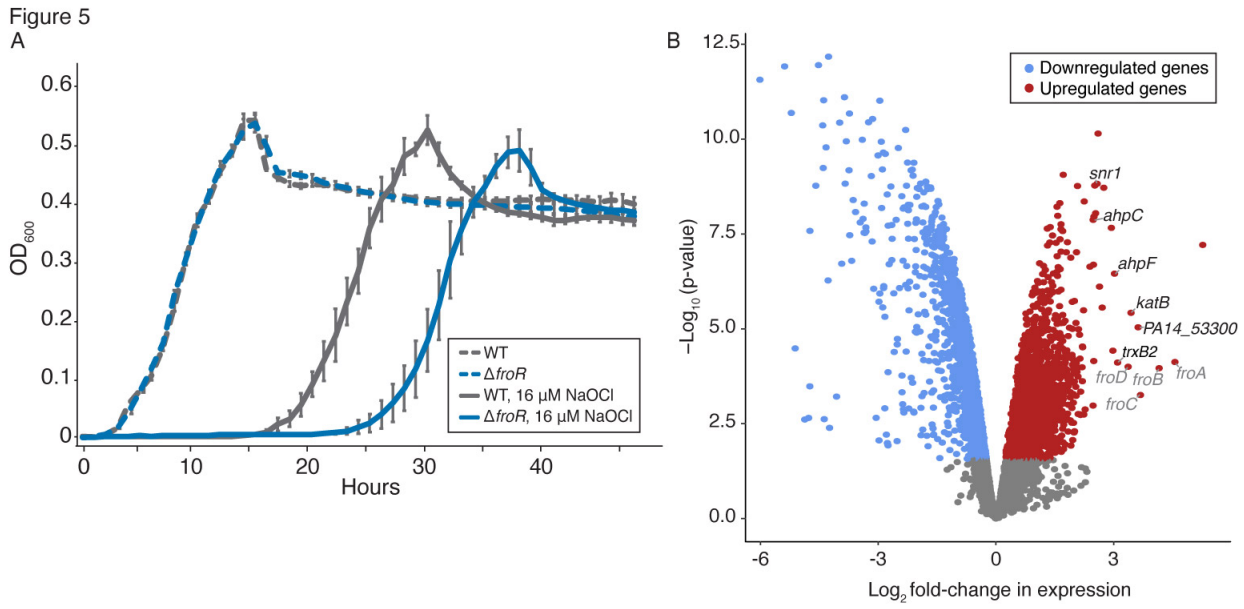

Fig. 5 FroR improves *P. aeruginosa* survival against HOCl stress and regulates the transcription of genes involved in antioxidant defense. (A) Growth profiles of wild-type (WT) *P. aeruginosa* and Δ*froR* mutants that were treated with 16 μM NaOCl or untreated. Data points represent the mean and the error bars indicate the SEM of three independent experiments. **(B)** Volcano plot indicating the fold-changes in transcripts and p-values of the wild-type (WT) strain relative to the Δ*froR* mutant using RNA-seq dataset from *(3)*. The colors reflect genes that are downregulated (blue), upregulated (red), or unchanged (grey) in WT strains compared to the Δ*froR* mutant. False discovery rate < 0.05.

Discussion

Neutrophils are activated by the presence of bacteria during the infection of host tissues. In this activated state, neutrophils produce respiratory bursts that contain high concentrations of HOCl. Whether and how bacteria respond to activated neutrophils and the RCS that the neutrophils produce has not been clear. In this study, we have demonstrated that *P. aeruginosa* responds to activated neutrophils by upregulating the transcriptional expression of the *fro* operon, which relieves HOCl-induced stress. Our data suggest that *fro* activation could function as a bacterial defense mechanism against a neutrophil attack mechanism. The *fro* response may

223 thus improve *P. aeruginosa* survival against neutrophils and enhance the colonization of human
224 tissues during infection.

225 One of the striking features of the *fro* system is that it is finely tuned to activate at sub-
226 lethal concentrations (1-2 μM) of NaOCl. Activated neutrophils produce HOCl as high as 50 μM
227 HOCl *(24)*. The activation of *fro* at relatively low concentrations suggests that the system
228 functions as a sensitive early detector of HOCl. In host environments, *fro* may activate in
229 environments where HOCl is present at low concentrations, such as during early stages of
230 neutrophil stimulation or when *P. aeruginosa* is spatially distant from activated neutrophils. The
231 early activation of *fro* could benefit *P. aeruginosa* by triggering a protective mechanism that
232 relieves the impact of HOCl stress before HOCl reaches lethal concentrations. This mechanism
233 would ensure that the system is already activated when *P. aeruginosa* encounters neutrophils.
234 Indeed, we observed that *fro* expression is strongly upregulated in *P. aeruginosa* that are in close
235 proximity to activated neutrophils (Fig. 1C). Additional evidence supports the function of *fro* as
236 a defensive early detection mechanism. The transcription of *fro* is partially activated by moving
237 fluids *(3)* that generate wall shear stresses in animal circulatory systems. Neutrophils move in the
238 fluidic networks of the circulatory system in response to tissue injury. *P. aeruginosa* that are
239 present in the circulatory system could prime its defenses via flowing sensing by *fro* against
240 potential HOCl produced by recruited neutrophils.

241 How does *fro* relieve HOCl stress in bacteria? The *fro* operon activates over 100 genes,
242 including *ahpC*, *ahpF*, and *katB,* that encode proteins that reduce the activity of ROS and are
243 critical for bacterial survival against oxidative stress (Fig. 5B) *(25, 26)*. While the effect of these
244 antioxidant proteins on RCS activity is unclear, our data suggest that *fro* activation mitigates the
245 toxic effects of HOCl (Fig. 5A). In addition, our results indicate that the presence of antioxidant

246 agents, including methionine, cysteine, or BME, reduces the activity of HOCl (Figs. 3-4).
247 Together, our data suggest a model in which *P. aeruginosa* senses HOCl via the *fro* system,
248 which upregulates the production of antioxidant proteins that suppress the toxic effects of HOCl.
249 This would constitute an early detection mechanism that defends against neutrophils. A recent
250 finding identified the RclR transcriptional regulator as a sensor of HOCl *(27)*. Further work is
251 necessary to determine how antioxidative proteins and antioxidative agents reduce the toxic
252 activity of HOCl and the extent that RclR and *fro* are co-regulated by HOCl.
253 In addition to promoting colonization of the lung and gastrointestinal tract *(13, 28)*, the
254 *fro* system may have additional impacts on pathogenicity, such as increasing antibiotic
255 resistance. Bacteria that are exposed to low doses of HOCl have higher rates of horizontal gene
256 transfer and can acquire antibiotic resistance genes more rapidly *(29, 30)*. The tolerance of
257 *P. aeruginosa* to HOCl via *fro* may thus provide a mechanism to facilitate antibiotic resistance.
258 The findings here thus suggest that the *fro* pathway could be an important defense mechanism to
259 target. Inhibition of this pathway could increase *P. aeruginosa* susceptibility to neutrophil-
260 mediated killing while minimizing antibiotic resistance.
261
262

263 **MATERIALS AND METHODS**

264

265 *Strains and Growth Conditions*

266 Experiments were performed using the *P. aeruginosa* strain AL143, which contains the
267 *yfp* gene integrated between *froA* and *froB* and a constitutively-expressed *mCherry* gene *(3)*. For
268 experiments with response of *P. aeruginosa* against NaOCl Δ*froR* and Δ*froI* mutant strains were
269 used *(3)*. Strains were streaked onto LB-Miller (BD Biosciences, Franklin Lakes, NJ) petri dishes
270 containing 2% Bacto agar (BD Biosciences, Franklin Lakes, NJ), incubated at 37 °C to obtain
271 single colonies, and inoculated into MinA minimal medium, which contains per 1 L of water:
272 4.5 g KH_2PO4, 10.5 g K_2HPO_4, 1 g $(NH_4)_2SO_4$, 1 mM $MgSO_4$ and 0.2 % (w/v) sodium citrate
273 *(31)*. Strains were cultured in minimal medium for 18 hours in a roller drum spinning at 200 rpm
274 at 37 °C, diluted 1:1000 into the same medium supplemented with oxidative or antioxidative
275 agents, conditioned medium from neutrophils, or were not supplemented, cultured for 1 hour at
276 37 °C, and imaged using microscopy.

277

278 *Phase Contrast and Fluorescence Microscopy*

279 Bacteria were immobilized on 1% agarose pads containing minimal medium and imaged
280 immediately. Images were acquired using a Nikon Eclipse Ti-E microscope (Nikon, Melville,
281 NY) containing a Nikon 100X Plan Apo (1.45 N.A.) objective, a Nikon Ph3 phase contrast
282 condenser annulus, a Sola light engine (Lumencor, Beaverton, OR), an LED-DA/FI/TX filter set
283 (Semrock, Rochester, NY) for visualizing the mCherry fluorescence spectrum containing a
284 409/493/596 dichroic and 575/25 nm filters for excitation and 641/75 nm filters for emission, an
285 LED-CFP/YFP/MCHERRY filter set (Semrock) for visualizing YFP fluorescence containing a

286 459/526/596 dichroic and 509/22 nm filters for excitation and 544/24 nm filters for emission,
287 and a Hamamatsu Orca Flash 4.0 V2 camera (Hamamatsu, Bridgewater, NJ).
288 Images were acquired using Nikon NIS-Elements and analyzed using custom built
289 software written previously *(32)* in Matlab (Mathworks, Natick, MA). See the "Code
290 availability" section below to download code. Briefly, cell masks were determined from phase
291 contrast images using an edge-detection algorithm. The YFP to mCherry fluorescence ratios in
292 the masked cell areas were computed. The expression of *fro* is quantified as the ratio of YFP to
293 mCherry fluorescence in individual *P. aeruginosa*, which is averaged over at least one hundred
294 *P. aeruginosa*. A minimum of 100 cells were imaged and analyzed in each experiment.
295
296 Imaging *P. aeruginosa* under flow
297 Microfluidic devices were fabricated using standard soft lithography techniques as
298 described previously *(33)* with channel dimensions of 100 µm x 50 µm (width x height) and a
299 flow rate of approximately 5 µL/min.
300
301 *Growth Curves*
302 Growth curve experiments were performed using a Synergy HTX multi-mode plate
303 reader and sterile, tissue-culture treated, clear bottom, black polystyrene 96-well microplates
304 (Corning, Corning, NY) containing 200 µL of culture in each well. The temperature set point
305 was 37 °C and preheated before beginning measurements. For experiments performed with
306 stationary phase bacteria, overnight cultures of bacteria were grown for 18 hours at 37 °C in the
307 roller drum at 200 rpm to saturation, diluted into minimal medium to an optical density at 600
308 nm (OD_{600}) of 0.01 containing NaOCl, H_2O_2, HNO_3 or no supplement. Plates were incubated at

309 37 °C with continuous orbital shaking with an amplitude of 3 mm at the frequency of 180 cycles
310 per minute and measured for OD_{600} every 20 minutes.
311
312 *Cell size analysis*
313 *P. aeruginosa* were cultured for 18 hours at 37 °C in a roller drum spinning at 200 rpm,
314 diluted 1:1000 into fresh minimal medium, treated 1 μM NaCl, 200 μM HCl or with serial
315 dilutions of NaOCl, H_2O_2, HNO_3 or media only, and incubated at 37 °C in 250 mL flasks for 3
316 hours with shaking at 225 rpm. Cells were immobilized on 1% agarose pads containing minimal
317 medium, imaged using phase contrast microscopy, and analyzed using the edge detection image
318 analysis tools in Matlab described above. The total pixel area of each individual cell was
319 determined by computing the mask area and converting from pixels to μm^2 by multiplying the
320 mask area by a factor of 0.004225 μm^2/pixel to account for the microscope camera pixel size and
321 objective magnification.
322
323 *Neutrophil isolation*
324 Blood samples from healthy donors between 18 to 65 years old were collected at the
325 Institute for Clinical and Translational Science at the University of California, Irvine, through
326 approved protocols with the UCI Institutional Review Board, and informed consent was obtained
327 from all donors. Neutrophils were prepared essentially as described in *(34)*. Briefly, 3% dextran
328 (Leuconostoc spp, Mr 450,000-650,000, Sigma-Aldrich, St. Louis, MO) in PBS (Gibco,
329 ThermoFisher, Waltham, MA) was used to separate red blood cells (RBCs) from whole blood.
330 Neutrophils were purified from the remaining cells by overlaying on a Ficoll density gradient

331 (GE Healthcare, Chicago, IL) following centrifugation in Ficoll-Paque Centrifugation Media
332 (GE Healthcare, Chicago, IL) for 25 minutes at 500 × g.
333 The remaining RBCs were lysed using RBC Lysis Buffer (Fisher Scientific, Hampton,
334 NH), and neutrophils were resuspended in RPMI 1640 medium (ATCC, Manassas, VA) and
335 purity was assessed by flow cytometry using the ACEA NovoCyte Flow Cytometer and
336 fluorescent antibodies APC-CD11b, FITC-CD16 and PE-CD66b (eBioscience, San Diego, CA).
337 Neutrophils were immediately used for neutrophil stimulation or co-incubation experiments with
338 *P. aeruginosa*. This procedure routinely yielded greater than 95% CD11B-positive neutrophil
339 populations.
340
341 *Tissue culturing*
342 J774.1 mouse macrophages (ATCC) or primary neonatal normal human dermal
343 fibroblasts (Neo-NHDF) (ATCC) were cultured in 10 mL DMEM (Gibco, ThermoFisher) in T75
344 flasks (VWR, Radnor, PA) at 37 °C with 5% CO_2. Macrophages were passaged every three days
345 through scraping and Neo-NHDF cells were passaged every 5 days through trypsinization.
346
347 *Co-incubation of mammalian cells with P. aeruginosa*
348 *P. aeruginosa* were cultured for 18 hours in minimal medium, centrifuged at 4600 x g for
349 2 minutes and resuspended in DPBS (Gibco, ThermoFisher) three times, and diluted to a final
350 OD_{600} of 0.2. Macrophages or Neo-NHDF cells that were harvested from growth flasks, or
351 freshly prepared neutrophils, were washed three times by centrifuging at 300 x g for 5 minutes
352 and resuspending in DPBS, and 1 mL aliquots containing 4 x 10^5 cells/mL were transferred into
353 flat-bottom dishes. *P. aeruginosa* culture was added to the cells at a multiplicity of infection of

354 10 and incubated at 37 °C with CO_2 for 30 minutes. Dishes were aspirated until approximately
355 20 µL of media remained and pads consisting of 1 % agarose containing DPBS were placed on
356 top of the samples in the dishes to immobilize bacteria and cells. Samples were imaged
357 immediately using microscopy.
358
359 *Preparation of neutrophil-stimulated conditioned medium*
360 Approximately 2 million/mL of freshly harvested neutrophils were incubated at 37 °C in a
361 roller drum spinning at a speed of 4 rotations per minute in PBGT medium (10 mM phosphate
362 buffer pH 7.4 (2.46 mM monobasic with 7.54 mM dibasic sodium phosphate), 140 mM sodium
363 chloride, 10 mM potassium chloride, 0.5 mM magnesium chloride, 1 mM calcium chloride, 1
364 mg/mL glucose, and 5 mM taurine *(24)*). Neutrophils were supplemented with 100 ng/mL of PMA
365 or left untreated for 1 hour, and were separated from the supernatant by 5 minute centrifugation at
366 4,600 x g at 25 °C. The supernatant was isolated and used as conditioned medium.
367 *P. aeruginosa* were cultured in minimal medium for 18 hours at 37 °C in a roller drum
368 spinning at 200 rpm, diluted 1:1000 in conditioned media with or without the addition of 100 µM
369 methionine, and incubated for 3 hours. Bacterial culture from each sample was concentrated using
370 cellulose syringe filters with a 0.22 µm pore size (Millipore, Burlington, MA). *P. aeruginosa* cells
371 were immobilized on 1% agarose pads and imaged. Data analysis was performed as described in
372 the "cell size analysis" methods section.
373
374 Antioxidant treatments
375 *P. aeruginosa* cultured for 18 hours at 37 °C in a roller drum spinning at 200 rpm, diluted
376 1:1000 into fresh minimal medium were diluted 1:1000 into minimal medium alone or

377 supplemented with 1 μM NaOCl with an addition of methionine (1 μM, 10 μM, 100 μM), β-
378 mercaptoethanol (βME) (1 μM, 10 μM, 100 μM) or cysteine (0.1 μM, 1 μM, 10 μM). 50 mL of
379 each bacterial culture was incubated at 37 °C in 250 mL flasks for 3 hours with shaking at 225
380 rpm. Data analyses were performed as described in the "cell size analysis" methods section
381 showed that the visible decrease of *fro* response to 1 μM NaOCl was observed when using 0.1
382 μM cysteine, 1 μM methionine and 1 μM βME. While *fro* response was not elevated at higher
383 concentrations of these antioxidants.
384
385 *Code Availability*
386 The custom Matlab scripts used to process and analyze the fluorescence microscopy data
387 have been previously described *(32)* and are freely available from Zenodo at
388 https://doi.org/10.5281/zenodo.3898289. Gene Ontology enrichment analysis was performed
389 using GOEnrichment version 2.0.1 *(35)*. The analysis of RNA-seq data was performed using
390 the limma Bioconductor package in Galaxy version 3.48.0 *(36)*.
391
392 **Supplementary Material**
393 Supplemental Figures S1-S3
394 Supplemental Spreadsheet 1
395 Supplemental Spreadsheet 2
396 Source Data file
397
398

399 **REFERENCES**

400 1. Centers for Disease Control and Prevention (U.S.), *Antibiotic resistance threats in the United*
401 *States, 2019* (Centers for Disease Control and Prevention (U.S.), 2019;
402 https://stacks.cdc.gov/view/cdc/82532).

403 2. F. C. Fang, E. R. Frawley, T. Tapscott, A. Vázquez-Torres, Bacterial Stress Responses during
404 Host Infection. *Cell Host Microbe* **20**, 133–143 (2016).

405 3. J. E. Sanfilippo, A. Lorestani, M. D. Koch, B. P. Bratton, A. Siryaporn, H. A. Stone, Z. Gitai,
406 Microfluidic-based transcriptomics reveal force-independent bacterial rheosensing. *Nat*
407 *Microbiol* **4**, 1274–1281 (2019).

408 4. E. G. Lavoie, T. Wangdi, B. I. Kazmierczak, Innate immune responses to Pseudomonas
409 aeruginosa infection. *Microbes Infect* **13**, 1133–1145 (2011).

410 5. A. W. Segal, How neutrophils kill microbes. *Annu Rev Immunol* **23**, 197–223 (2005).

411 6. M. B. Hampton, A. J. Kettle, C. C. Winterbourn, Inside the neutrophil phagosome: oxidants,
412 myeloperoxidase, and bacterial killing. *Blood* **92**, 3007–3017 (1998).

413 7. F. C. Fang, Antimicrobial actions of reactive oxygen species. *mBio* **2** (2011),
414 doi:10.1128/mBio.00141-11.

415 8. M. J. Gray, W.-Y. Wholey, U. Jakob, Bacterial responses to reactive chlorine species. *Annu*
416 *Rev Microbiol* **67**, 141–160 (2013).

417 9. C. Estrela, R. G. Ribeiro, C. R. A. Estrela, J. D. Pécora, M. D. Sousa-Neto, Antimicrobial
418 effect of 2% sodium hypochlorite and 2% chlorhexidine tested by different methods. *Braz Dent J*
419 **14**, 58–62 (2003).

420 10. J. M. Albrich, J. K. Hurst, Oxidative inactivation of Escherichia coli by hypochlorous acid.
421 Rates and differentiation of respiratory from other reaction sites. *FEBS Lett* **144**, 157–161
422 (1982).

423 11. J. E. Harrison, J. Schultz, Studies on the chlorinating activity of myeloperoxidase. *J Biol*
424 *Chem* **251**, 1371–1374 (1976).

425 12. E. T. Jensen, A. Kharazmi, K. Lam, J. W. Costerton, N. Høiby, Human polymorphonuclear
426 leukocyte response to Pseudomonas aeruginosa grown in biofilms. *Infect Immun* **58**, 2383–2385
427 (1990).

428 13. E. Potvin, D. E. Lehoux, I. Kukavica-Ibrulj, K. L. Richard, F. Sanschagrin, G. W. Lau, R. C.
429 Levesque, In vivo functional genomics of Pseudomonas aeruginosa for high-throughput
430 screening of new virulence factors and antibacterial targets. *Environ Microbiol* **5**, 1294–1308
431 (2003).

432 14. D. M. Cornforth, J. L. Dees, C. B. Ibberson, H. K. Huse, I. H. Mathiesen, K. Kirketerp-
433 Møller, R. D. Wolcott, K. P. Rumbaugh, T. Bjarnsholt, M. Whiteley, Pseudomonas aeruginosa
434 transcriptome during human infection. *Proc Natl Acad Sci U S A* **115**, E5125–E5134 (2018).

435 15. G. L. Winsor, E. J. Griffiths, R. Lo, B. K. Dhillon, J. A. Shay, F. S. L. Brinkman, Enhanced
436 annotations and features for comparing thousands of Pseudomonas genomes in the Pseudomonas
437 genome database. *Nucleic Acids Res* **44**, D646-653 (2016).

438 16. A. L. Boechat, G. H. Kaihami, M. J. Politi, F. Lépine, R. L. Baldini, A novel role for an ECF
439 sigma factor in fatty acid biosynthesis and membrane fluidity in Pseudomonas aeruginosa. *PLoS*
440 *One* **8**, e84775 (2013).

441 17. A. Karlsson, J. B. Nixon, L. C. McPhail, Phorbol myristate acetate induces neutrophil
442 NADPH-oxidase activity by two separate signal transduction pathways: dependent or
443 independent of phosphatidylinositol 3-kinase. *J Leukoc Biol* **67**, 396–404 (2000).

444 18. K. V. Farrant, L. Spiga, J. C. Davies, H. D. Williams, Response of Pseudomonas aeruginosa
445 to the Innate Immune System-Derived Oxidants Hypochlorous Acid and Hypothiocyanous Acid.
446 *J Bacteriol* **203**, e00300-20 (2020).

447 19. C. C. Winterbourn, Comparative reactivities of various biological compounds with
448 myeloperoxidase-hydrogen peroxide-chloride, and similarity of the oxidant to hypochlorite.
449 *Biochim Biophys Acta* **840**, 204–210 (1985).

450 20. D. I. Pattison, M. J. Davies, Reactions of myeloperoxidase-derived oxidants with biological
451 substrates: gaining chemical insight into human inflammatory diseases. *Curr Med Chem* **13**,
452 3271–3290 (2006).

453 21. G. Atmaca, Antioxidant effects of sulfur-containing amino acids. *Yonsei Med J* **45**, 776–788
454 (2004).

455 22. C. L. Hawkins, D. I. Pattison, M. J. Davies, Hypochlorite-induced oxidation of amino acids,
456 peptides and proteins. *Amino Acids* **25**, 259–274 (2003).

457 23. P. Bin, R. Huang, X. Zhou, Oxidation Resistance of the Sulfur Amino Acids: Methionine and
458 Cysteine. *Biomed Res Int* **2017**, 9584932 (2017).

459 24. J. M. Dypbukt, C. Bishop, W. M. Brooks, B. Thong, H. Eriksson, A. J. Kettle, A sensitive
460 and selective assay for chloramine production by myeloperoxidase. *Free Radic Biol Med* **39**,
461 1468–1477 (2005).

462 25. L. C. Seaver, J. A. Imlay, Alkyl hydroperoxide reductase is the primary scavenger of
463 endogenous hydrogen peroxide in Escherichia coli. *J Bacteriol* **183**, 7173–7181 (2001).

464 26. S. M. Brown, M. L. Howell, M. L. Vasil, A. J. Anderson, D. J. Hassett, Cloning and
465 characterization of the katB gene of Pseudomonas aeruginosa encoding a hydrogen peroxide-
466 inducible catalase: purification of KatB, cellular localization, and demonstration that it is
467 essential for optimal resistance to hydrogen peroxide. *J Bacteriol* **177**, 6536–6544 (1995).

468 27. K. V. Farrant, L. Spiga, J. C. Davies, H. D. Williams, Response of Pseudomonas aeruginosa
469 to the Innate Immune System-Derived Oxidants Hypochlorous Acid and Hypothiocyanous Acid.
470 *J Bacteriol* **203**, e00300-20 (2020).

471 28. D. Skurnik, D. Roux, H. Aschard, V. Cattoir, D. Yoder-Himes, S. Lory, G. B. Pier, A
472 comprehensive analysis of in vitro and in vivo genetic fitness of Pseudomonas aeruginosa using
473 high-throughput sequencing of transposon libraries. *PLoS Pathog* **9**, e1003582 (2013).

474 29. A.-M. Hou, D. Yang, J. Miao, D.-Y. Shi, J. Yin, Z.-W. Yang, Z.-Q. Shen, H.-R. Wang, Z.-G.
475 Qiu, W.-L. Liu, J.-W. Li, M. Jin, Chlorine injury enhances antibiotic resistance in Pseudomonas
476 aeruginosa through over expression of drug efflux pumps. *Water Res* **156**, 366–371 (2019).

477 30. M. Jin, L. Liu, D. Wang, D. Yang, W. Liu, J. Yin, Z. Yang, H. Wang, Z. Qiu, Z. Shen, D.
478 Shi, H. Li, J. Guo, J. Li, Chlorine disinfection promotes the exchange of antibiotic resistance
479 genes across bacterial genera by natural transformation. *ISME J* **14**, 1847–1856 (2020).

480 31. H. Malke, Jeffrey H. Miller, A Short Course in Bacterial Genetics – A Laboratory Manual
481 and Handbook forEscherichia coli and Related Bacteria. Cold Spring Harbor 1992. Cold Spring
482 Harbor Laboratory Press. ISBN: 0–87969-349–5. *J Basic Microbiol* **33**, 278–278 (1993).

483 32. T. Doolin, H. M. Amir, L. Duong, R. Rosenzweig, L. A. Urban, M. Bosch, A. Pol, S. P.
484 Gross, A. Siryaporn, Mammalian histones facilitate antimicrobial synergy by disrupting the
485 bacterial proton gradient and chromosome organization. *Nat Commun* **11**, 3888 (2020).

486 33. A. Siryaporn, M. K. Kim, Y. Shen, H. A. Stone, Z. Gitai, Colonization, competition, and
487 dispersal of pathogens in fluid flow networks. *Curr Biol* **25**, 1201–1207 (2015).

488 34. H. L. Clark, S. Abbondante, M. S. Minns, E. N. Greenberg, Y. Sun, E. Pearlman, Protein
489 Deiminase 4 and CR3 Regulate Aspergillus fumigatus and β-Glucan-Induced Neutrophil
490 Extracellular Trap Formation, but Hyphal Killing Is Dependent Only on CR3. *Front Immunol* **9**,
491 1182 (2018).

492 35. Gene Ontology Consortium, The Gene Ontology resource: enriching a GOld mine. *Nucleic*
493 *Acids Res* **49**, D325–D334 (2021).

494 36. C. W. Law, Y. Chen, W. Shi, G. K. Smyth, voom: Precision weights unlock linear model
495 analysis tools for RNA-seq read counts. *Genome Biol* **15**, R29 (2014).

496

497

498 **Acknowledgments:** The authors thank Michael Z. Zulu and Stephanie Matsuno for their
499 feedback on prior drafts of this article and Hew Yeng Lai for imaging of bacteria in microfluidic
500 devices. **Funding:** This work was supported by the Stanley Behrens Fellows in Medicine Award
501 to L.U, and grants from the National Institutes of Health (NIH) National Institute of Biomedical
502 Imaging and Bioengineering (NIBIB) (R21EB027840-01), the National Cancer Institute (NCI)
503 (DP2CA250382-01), the National Science Foundation (NSF) (DMS1763272), and a grant from
504 the Simons Foundation (594598QN) to T.L.D. **Author contributions:** I.F. and A.S. conceived
505 and designed the experiments. I.F. and A.H. performed the experiments. L.U. prepared
506 neutrophils from human samples. I.F. and L.U. analyzed data and wrote the initial draft of the
507 paper. I.F., L.U., T.L.D., and A.S. discussed results and edited the paper. **Competing interests:**
508 Authors declare that they have no competing interests. **Data and materials availability:** Raw
509 data for all figures that contain t-test analyses are available in the Supplementary Information
510 Source Data file.
511

Supplementary Material

Supplemental Figures S1-S3
Supplemental Spreadsheet 1 (Microsoft Excel format)
Supplemental Spreadsheet 2 (Microsoft Excel format)
Source Data file (Microsoft Excel format). Contains raw data and statistics for main and supplemental figures

Supplemental Figure S1

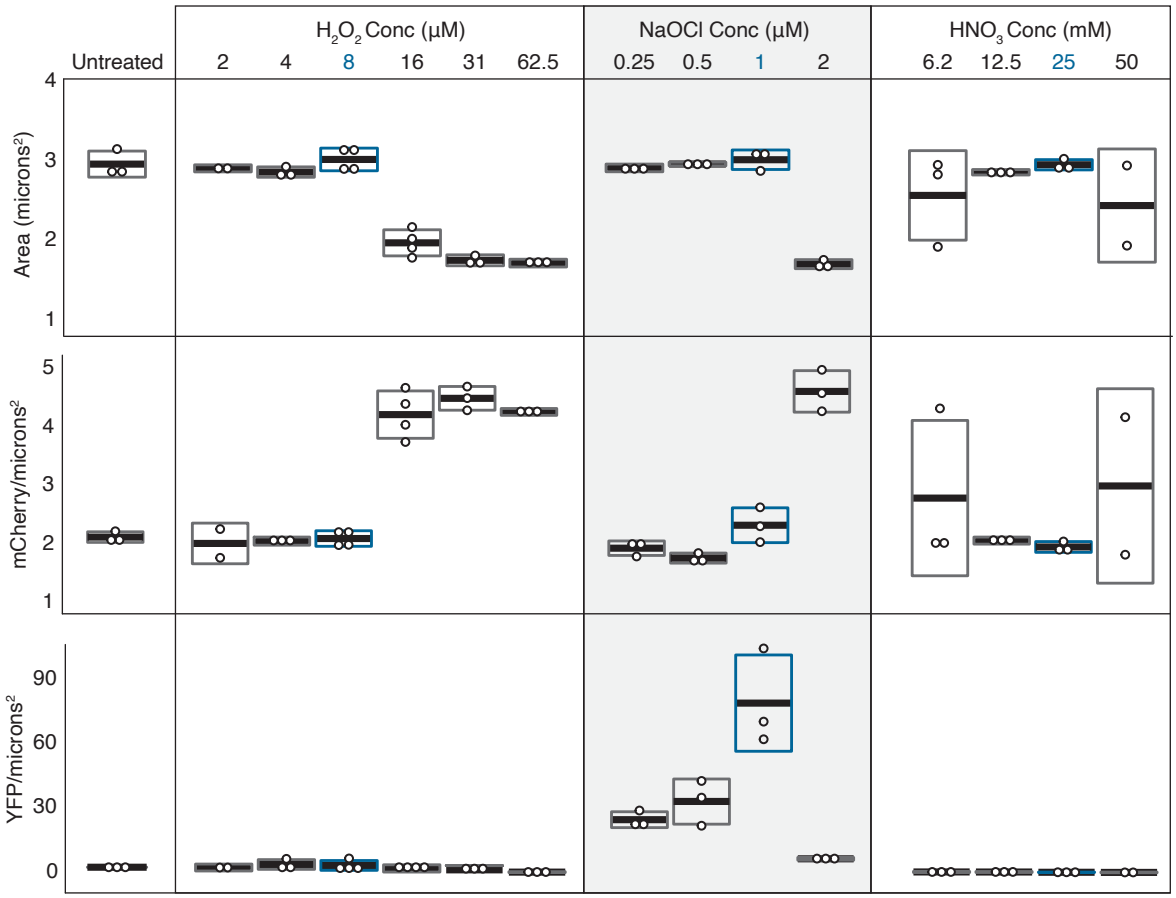

Fig. S1 Effects on cell size and global transcription in *P. aeruginosa* treated with NaOCl, H_2O_2, or HNO_3. Top: average area of individual *P. aeruginosa* cells, Middle: average mCherry/area, Bottom: average YFP/area in *P. aeruginosa* treated with dilutions of H2O2, NaOCl, HNO3, or untreated for 3 hours. Boxplots show the mean (black line) and the interquartile range of three independent experiments. Blue boxes indicate the datasets that were used to compute the values for Fig. 3D.

Supplemental Figure S2

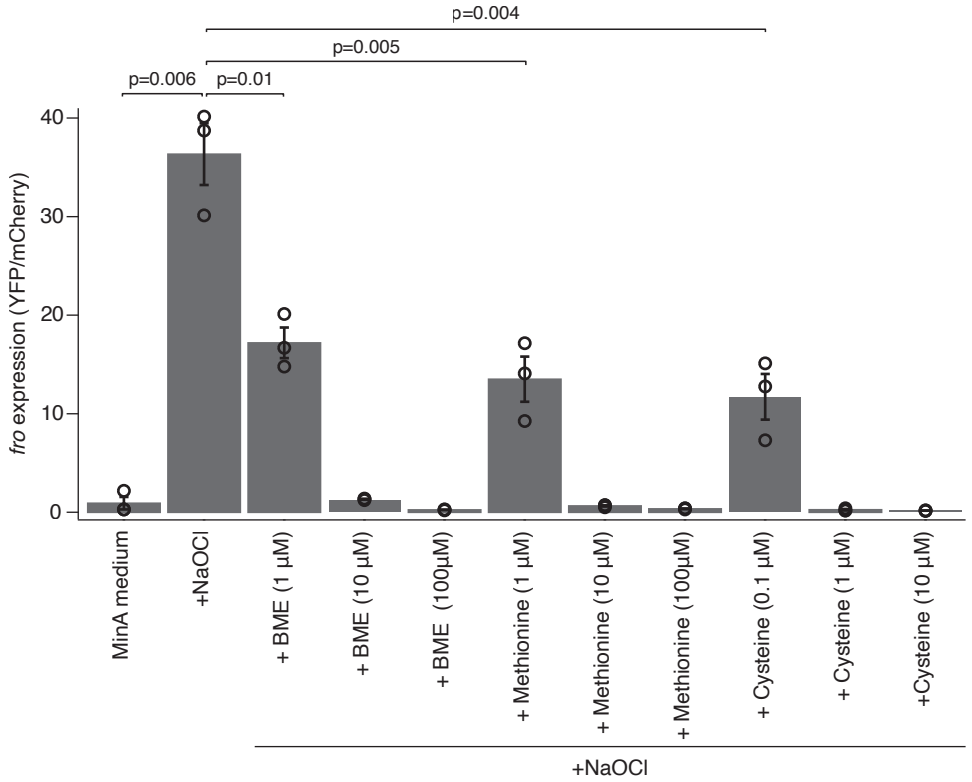

Fig. S2. Dose-dependent effects of antioxidant supplements on *fro* expression induced by HOCl. Quantification of *fro* expression levels in *P. aeruginosa* cultures treated with 1 µM NaOCl and supplemented with methionine, cysteine, or beta-mercaptoethanol (BME). Plots show the mean and SEM for three independent experiments. P-values were calculated using two-tailed, unequal variance t-test. ns indicates $p > 0.05$.

Supplemental Figure S3

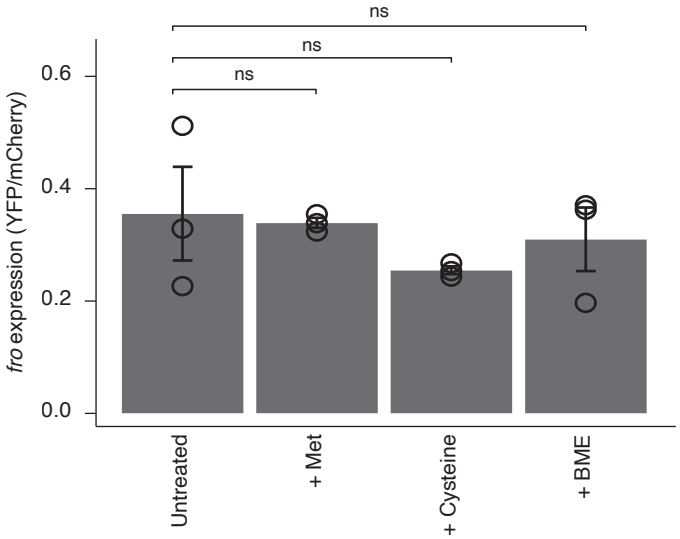

Fig. S3. Effects of antioxidants alone on *fro* expression. Quantification of *fro* expression levels in *P. aeruginosa* cultures treated with 1 µM methionine, 0.1 µM cysteine, 1 µM beta-mercaptoethanol (BME), or untreated (MinA data replotted from Fig. 3C). Plots show the mean and the standard error of the mean (SEM) for three independent experiments. P-values were calculated using two-tailed, unequal variance t-test. ns indicates $p > 0.05$.